Mechanism and Kinetics of Transfer of a Fluorescent Fatty Acid between Single-Walled Phosphatidylcholine Vesicles†

Michael C. Doody,‡ Henry J. Pownall,§ Yin J. Kao,‡ and Louis C. Smith*

ABSTRACT: The transfer of a fatty acid, 9-(3-pyrenyl)nonanoic acid (PNA), between synthetic phospholipid single-bilayer vesicles is a first-order process, with no dependence on either the concentrations of donor and acceptor vesicles or the chemical composition of acceptor vesicles. The invariance in transfer rates over 50-fold change in concentration of vesicles and an identical rate constant for transfer of the fluorescent fatty acid from vesicles to solution is compelling evidence that the transfer of PNA between phospholipid vesicles proceeds through the aqueous phase. High ionic strength, 4 M NaCl, reduces the reaction rate 25–60-fold, depending on the pH and temperature. The rate of transfer of ionized PNA is faster than that of the protonated form. At 28 °C and pH 7.4, the rate constant for transfer of PNA between dimyristoylphosphatidylcholine is 5.4 s^{-1}; at pH 2.8, it is 0.08 s^{-1}. Between pH 2.8 and 7.4, observed rates are the arithmetic sum of the rates of protonated and ionized PNA; transbilayer "flip-flop" appears to be faster than transfer between vesicles. The activation energy for this process is determined by donor lipid phase and by the ionization state of the fatty acid. The activation energy for PNA transfer is lower below the transition temperature of the donor lipid vesicle than it is above it. The difference in the activation energy above and below the transition temperature is the same at pH 2.8 and 7.4. Arrhenius plots for transfer for protonated and ionized PNA show that the activation energy includes energies to offset phase-dependent and phase-independent free energies of association for the aryl–alkyl side chain and excess free energy of association of the protonated carboxyl group and the vesicle. Thermodynamics of the transition state and distribution parameters indicate that the rate-limiting step appears to be the solvation of PNA in the interfacial water at the phospholipid surface. Furthermore, the calculated pK_a of the activated state molecule is that of an aqueous carboxyl group, about 4.5. From kinetic considerations, the pK_a of the fatty acid in the phospholipid vesicle is 7.1. An excess free energy of association between the protonated carboxyl and the phospholipid membrane accounts for a 100-fold suppression of PNA ionization. The fatty acid anion is the chemical entity that transfers at physiological pH. These results imply that the properties of interfacial water limit the transfer rates of hydrophobic compounds between membrane surfaces.

The mechanism for transfer of fatty acid between membranes and lipoproteins has considerable importance as a potential rate-limiting step in the intravascular metabolism of triglyceride. The action of lipoprotein lipase on very low density lipoproteins and chylomicrons releases large amounts of fatty acid at the lipoprotein surface (Robinson, 1970; Scow et al., 1972). Little is known, however, about the precise mechanism of transfer or the time frame for movement of fatty acyl moieties between these lipoprotein surfaces. By undefined processes, most of these fatty acids migrate across the capillary endothelial cells into the underlying somatic cells for storage or utilization. Lateral movement of the fatty acids in cell membranes, albumin-mediated transfer of the fatty acids across the interstitial spaces, transient fusion of lipid surfaces, and transmembrane flip-flop have been proposed as possible routes for the translocation of fatty acids (Smith & Scow, 1979). To gain a better understanding of the overall reaction of triglyceride clearance at the capillary endothelial surface, we have investigated the kinetics and mechanism of transfer of a fluorescent fatty acid between model phospholipid membranes.

Ideally, studies of lipid transfer should give information not only about the time course and mechanism of the transfer phenomenon but also about the noncovalent interactions between the membrane surfaces and the molecule being transferred. The spectral properties of a novel fluorescent fatty acid, 9-(3-pyrenyl)nonanoic acid[1] (PNA), allow quantification of the distribution between the membrane and the aqueous phase, the rate of exchange, and the interaction of the fatty acid with host phospholipid matrix. Two other pyrene-substituted lipids synthesized in this laboratory have been used successfully to study the mechanism of lipid transfer (Charlton et al., 1978; Kao et al., 1977).

Following absorption of light, an excited singlet-state molecule (monomer) of pyrene and many pyrene derivatives can form an excited-state dimer (excimer) by collision with a ground-state pyrenyl moiety (Birks, 1970) (Figure 1). Ground-state PNA (I) can absorb light (for example, at 350 nm) to form the excited-state singlet molecule (II). The excited state can lose energy by three pathways. Pathway A is the direct fluorescence emission of pyrene at 390 nm of the energy left after Franck–Condon equilibration. Pathway B involves collision of the pyrene excited singlet state with a ground-state pyrene molecule to form the excimer complex (III). By pathway C, there is nonradiative thermal loss of the energy. The *excited*-state *dimer* or *excimer* can then lose energy either through nonradiative thermal loss or as fluorescence at a longer, characteristic wavelength at 470 nm. The ratio of excimer and monomer intensities is proportional

† From the Division of Atherosclerosis and Lipoprotein Research, Departments of Medicine and Biochemistry, Baylor College of Medicine and the Methodist Hospital, Houston, Texas 77030. *Received June 15, 1979.* Support was provided by Robert A. Welch Foundation Grant Q-343, the National Heart and Blood Vessel Research and Demonstration Center, Baylor College of Medicine, a grant-supported research project of the National Heart, Lung and Blood Institute, HL-17269, and U.S. Public Health Service Grants HL-15648 and HL-19459.

‡ Predoctoral Fellow of the Robert A. Welch Foundation.

§ Established Investigator of the American Heart Association.

[1] Abbreviations used: PNA, 9-(3-pyrenyl)nonanoic acid; PNOL, 9-(3-pyrenyl)nonanol; I_E, relative intensity of excimer fluorescence; I_M, relative intensity of monomer fluorescence; DMPC, dimyristoylphosphatidylcholine; DPPC, dipalmitoylphosphatidylcholine; T_m, gel → liquid-crystalline phase transition temperature; LC, high-performance liquid chromatography.

0006-2960/80/0419-0108$01.00/0

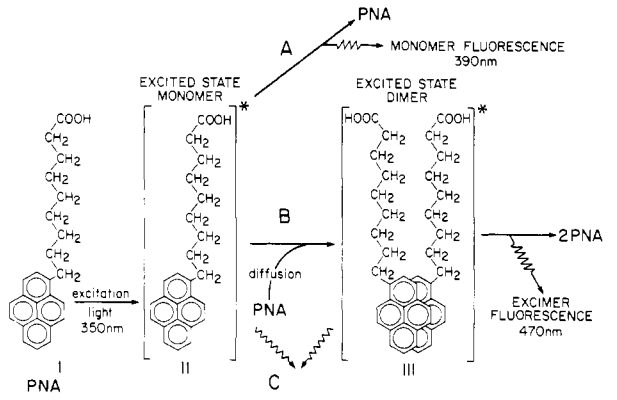

FIGURE 1: Photophysics of excimer fluorescence of 9-(3-pyrenyl)-nonanoic acid.

to the microscopic concentration of the probe and inversely proportional to the viscosity of the environment (Pownall & Smith, 1973). At low I_E/I_M ratios, changes in I_E are directly proportional to changes in the microscopic concentration of the pyrenyl group. These relationships are described by the equation

$$I_E/I_M = [\text{PNA}]TK/\eta \quad (1)$$

where T is the temperature in kelvin, K incorporates both theoretical and instrumental constants, and η is the viscosity (Soutar et al., 1974). In addition to the attractive fluorescence properties, pyrene is hydrophobic with low solubility in water (Almgren et al., 1979). For these reasons properly substituted pyrene derivatives are ideal for studying lipid exchange (Charlton et al., 1978; Kao et al., 1977).

In a limited study of fatty acid transfer, Sengupta et al. (1976) found that the transfer of 10-(3-pyrenyl)decanoic acid between artificial membranes is a first-order process. The transfer was examined in unbuffered solutions only at one probe and phospholipid concentration, and there was little experimental detail. A detailed study of the transfer mechanism was deemed necessary, in view of the metabolic importance of fatty acid transfer. An abstract of this work has appeared (Doody et al., 1978).

Experimental Procedures

Materials. DMPC and DPPC were purchased from Sigma Chemical Co. (St. Louis). DMPC was purified on a Waters preparative liquid chromatograph with a silica column in chloroform–ethanol–water (60:30:4 v/v). Residual myristic acid and monomyristoylphosphatidylcholine were absent in the purified lipid, judged by analytical LC in the same solvent system, by using a refractive index detector (Patel & Sparrow, 1978). DPPC was sufficiently pure by this criteria for use as received.

9-(3-Pyrenyl)nonanoic acid (PNA) was prepared by Friedel-Crafts acylation of 100 mmol of pyrene with an equimolar amount of the acyl chloride of monomethylazelaic acid in nitrobenzene. Wolff–Kishner reduction of the resulting keto ester, followed by hydrolysis with KOH and 18-crown-6 in benzene (Patel et al., 1976) and purification by preparative LC on silica column in hexane–ethyl acetate (6:4 v/v), gave 10 mmol of PNA in poor yield. The corresponding alcohol was prepared by reduction of PNA with sodium bis(methoxyethoxy)aluminum hydride (Redal, Alrich Chemical Co.) in benzene, with subsequent isolation of the product by preparative LC on silica in hexane–ethyl acetate (9:1 v/v). The electron impact mass spectrum of 9-(3-pyrenyl)nonanol is consistent with the proposed structure for PNA and the derived alcohol: m/e (rel abundance) 344 (M, 65.2), 330 (4.7), 327 (0.5), 241 (1.5), 228 (3.7), 215 (100), 202 (3.6). All lipids and fluorescent probes were stored in glass-distilled chloroform (Burdick & Jackson) at −15 °C. Other reagents and solvents were the best commercial grade.

Single-walled phosphatidylcholine vesicles were prepared by ethanol injection (Batzri & Korn, 1973). Final ethanol concentrations were adjusted to 2% v/v. When present, PNA or PNOL was dissolved in the ethanolic solution of phospholipid before injection into buffer. Except for the experiment in Figure 7, single-walled vesicles were used exclusively. For the experiment in Figure 7, multilamellar liposomes were prepared by the method of Bangham et al. (1965). When present, PNA or PNOL was added to the chloroform solution of the phospholipid. After the solvent was evaporated under N_2, residual chloroform was removed by mechanical vacuum for 1 h. Buffer, pH 7.4, was added with vortexing, and the mixture was allowed to stand at 37 °C for 2 h. The liposomes were separated with a pipet from any precipitate and used without correction for any change in the concentration.

For the pH range 2.8–6.4, the buffers contained 10 mM sodium acetate, 0.15 M NaCl, and 1 mM EDTA; for the pH range 7.4–9.0, the buffers contained 50 mM Tris, 0.15 M NaCl, and 1 mM EDTA. Water was double distilled from quartz. Solutions were degassed by water aspirator vacuum prior to use. Determination of the partition coefficients was done in NaBr rather than NaCl.

Methods. The stopped-flow apparatus and its use in determining transfer rates of pyrene containing lipids have been described previously (Charlton et al., 1976, 1978). In all cases the transfer rates are the average of three to five transfer traces. Exposure to excitation light at 350 nm was minimized to reduce photodecomposition, which was less than 1–2%. Exciting light was shuttered in the slower reactions.

Static fluorescence spectra were recorded on a Farrand Mark I spectrofluorometer with a 10-nm band-pass for both excitation and analyzing monochromators. An SLM Model 8000 digital single photon counting spectrofluorometer/polarimeter was used in the partitioning experiments. Absorption spectra were measured on a Cary 15 spectrophotometer. Constant temperature was maintained with a Lauda circulating bath. Spectra were recorded on a Houston Instruments Omnigraphic X–Y recorder.

Results

Fluorescence Behavior of PNA in DMPC Vesicles. The relationship between the ratio of excimer to monomer fluorescence and PNA concentration in DMPC vesicles was linear at both high and low pH values (Figure 2). The ratio decreased proportionately immediately when unlabeled vesicles were added to a solution of labeled vesicles. For example, when equimolar amounts of acceptor vesicles were added, the I_E/I_M ratio was halved. No additional time-dependent changes over 24 h were observed by this static method. With a 10-fold excess of acceptor vesicles, excimer fluorescence was essentially abolished within the mixing time. These results demonstrate that the probe transferred completely between vesicles.

Absorption spectra were measured to detect possible concentration-dependent behavior of the probe (Vanderkooi & Callis, 1974). No spectral evidence of phase separation of PNA in DMPC vesicles at 20 °C was found up to 15 mol % PNA. At 20 mol %, hypochromic spectral perturbation suggested cluster formation. Concentrations of 2 mol % PNA or less were used in all transfer experiments.

Since excimer formation is also influenced by temperature-dependent changes in microviscosity, the interaction of

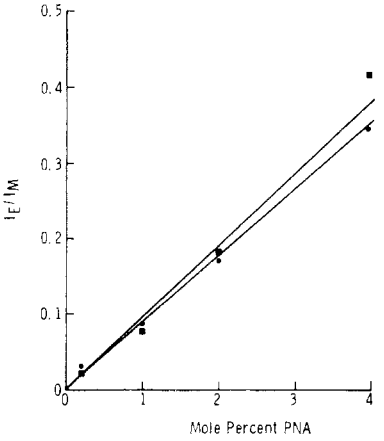

FIGURE 2: Relationship between I_E/I_M and PNA concentration in DMPC. I_E was measured at 470 nm and I_M was measured at 390 nm. A series of DMPC single-bilayer vesicle preparations at 0.2 mg/mL were labeled with the indicated amounts of probe at pH 2.8 (■) and 7.4 (●). The temperature was 21 °C. Other experimental details are given under Experimental Procedures.

PNA with the phospholipid matrix vesicles and the fluorescence ratio at different temperatures were determined. The probe was sensitive to phase change, as expected from previous reports of temperature-dependent and lipid phase dependent changes in microviscosity of phospholipid bilayers (Soutar et al., 1974; Vanderkooi & Callis, 1974; Galla & Sackman, 1974). The characteristic phase transition of DMPC was detected as a discontinuity in plots at about 20–24 °C at both pH 2.8 and pH 7.4, in agreement with changes in light scattering observed with phospholipid vesicles prepared by this method (Van Dijck et al., 1978). At pH 2.8, the phase transition of DMPC was not appreciably different from that seen at pH 7.4. Fluorescence polarization in these phospholipid vesicles labeled with *β-all-trans*-parinaric acid (Sklar et al., 1977) revealed a broad phase transition centered at ~24 °C. Ethanol at these concentrations had no detectable effect on the phase transition of DMPC or DPPC multilayers. DMPC and DPPC vesicles prepared by this method have thermal transitions at temperatures close to those of the corresponding multilamellar species.

pH Dependence of PNA Transfer. The results of a typical stopped-flow experiment are shown in Figure 3. The instrumental analogue outputs of a single mixing experiment illustrates the exponential decrease in excimer fluorescence and the corresponding linear logarithmic decay from which half-times for the transfer were obtained. The rate constant for transfer with changing pH was a sigmoidal function that approached constant values at both low pH and neutral pH (Figure 4). At these extremes of pH, fatty acid was assumed to exist entirely as either the protonated acid or the anion, respectively. At 34 °C, rate constants of 9.8 s^{-1} for the ionized form and 0.17 s^{-1} for the protonated form of PNA were observed.

Over the entire range between pH 2.8 and pH 7.4, a single-exponential decay that extended over at least 3 half-lives was observed. Since the concentration dependence of I_E/I_M was identical for both forms of PNA (Figure 2), the observed first-order kinetics for transfer reflected the summation of transfer rates for the rapidly equilibrating protonated and unprotonated forms of the *total* PNA population bound to the vesicle. The magnitude of the decreases in fluorescence intensities in these experiments corresponded to that determined in static experiments. The equilibration of the proton between the two forms was very fast (Eigen et al., 1964) compared to

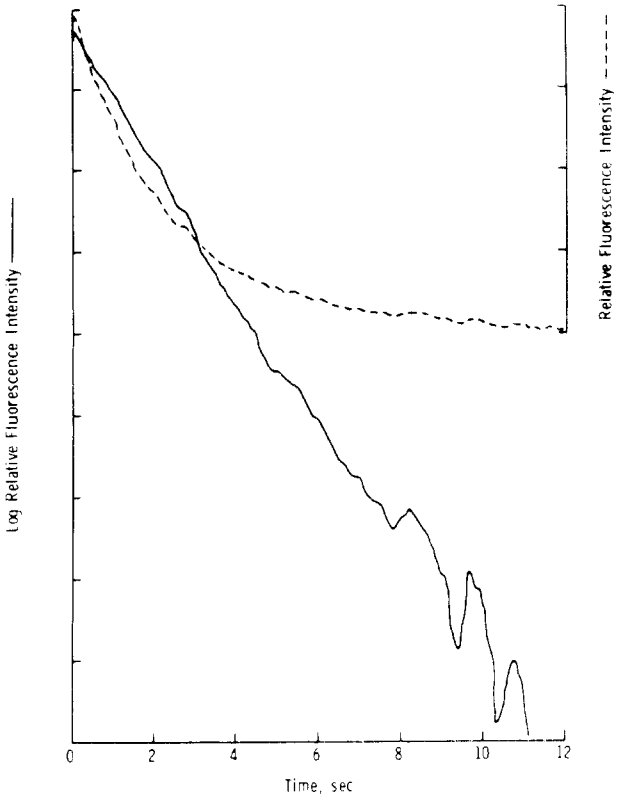

FIGURE 3: Trace for transfer of PNA between DMPC vesicles. The digital to analogue output from the decay excimer fluorescence intensity (- - -) and the log [excimer intensity (at time t) − excimer intensity (at ∞ time)] (—) is shown in arbitrary instrumental units. Rate constants and half-times were calculated from the slope of the exponential plots. The concentration of donor and acceptor DMPC vesicles was 0.28 mM at 34 °C; donor vesicles were labeled with 2 mol % PNA. The experiment was done at pH 5.1.

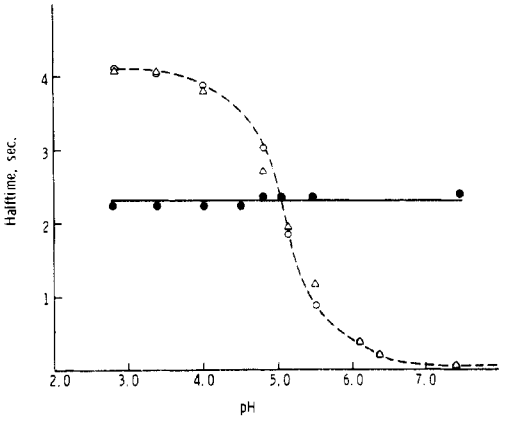

FIGURE 4: pH dependence of the half-time for transfer of PNA and PNOL between DMPC vesicles. Experimentally determined points for PNA (○) and PNOL (●) are shown. Theoretical values for PNA (△) calculated for each experimental point, as described in the text, are shown. Conditions, except for pH, were those described in the legend to Figure 3.

transfer, so that a biexponential exchange trace was not observed.

The large decrease of transfer at the low pH values could arise from pH-induced perturbation of the phospholipid bilayer rather than being the result of extent of ionization of the probe. The transfer of a nonionizing fatty acid analogue of PNA, 9-(3-pyrenyl)nonanol (PNOL), eliminated pH-induced changes of the phospholipid as a possible explanation. Within the range of experimental error, pH had no effect on the rate of transfer of this nonionizable fluorescent analogue of the

Table I: Effect of Donor and Acceptor Vesicle Concentration on Transfer of PNA between DMPC Vesicles at pH 2.8 and 7.4[a]

	initial concn of DMPC vesicles		
pH	donor (mM)	acceptor (mM)	half-time (ms)
7.4	0.014	0.0	91
7.4	0.014	0.014	91
7.4	0.07	0.07	97
7.4	0.14	0.14	99
7.4	0.71	0.71	92
2.8	0.007	0.0	NM[b]
2.8	0.014	0.014	4600
2.8	0.07	0.07	4500
2.8	0.14	0.14	4500
2.8	0.71	0.71	4300

[a] Rates of exchange are the average of three to five exchange traces. Rates of transfer to buffer were determined with 10:1 dilution syringes. In all other experiments, equal volumes of donor and acceptor solutions were mixed. Solutions were equilibrated at 30.5 °C within the instrument for 30 min before the kinetic experiments. Donor vesicles contained 2 mol % PNA. A low signal to noise ratio and the relatively long transfer time precluded accurate measurement of transfer rate at pH 2.8 in the absence of an acceptor vesicle, although a small decrease in excimer fluorescence was observed. [b] NM, not measurable.

Table II: Effect of Chemical Composition of Donor and Acceptor Vesicles on Transfer Lifetimes[a]

pH	donor	acceptor	half-time (ms)
7.4	DMPC	DMPC	42
7.4	DMPC	DPPC	41
7.4	DPPC	DMPC	48
7.4	DPPC	DPPC	45
2.8	DMPC	DMPC	4300
2.8	DMPC	DPPC	4200
2.8	DPPC	DMPC	2700
2.8	DPPC	DPPC	2700

[a] Equal concentrations of donor and acceptor vesicles at 0.284 mM were mixed at 37 °C. Other experimental details are found in the legend to Table I.

protonated form of PNA (Figure 4). The half-time for transfer of PNOL was 2.3 s^{-1} at pH 2.8 and 2.5 s^{-1} at pH 7.4, with similar half-times at intervals between these two pH limits. This experiment demonstrated that the ionization state of PNA accounted for the 50-fold difference in exchange rates at low and neutral pH.

Concentration Independence of PNA Transfer. Within the range of experimental error, the rate of transfer was independent of the concentrations of both donor and acceptor vesicles over a 50-fold range at both pH 2.8 and pH 7.4 (Table I). PNA also was transferred from the donor particles to the aqueous solution when low concentrations of vesicles were diluted an additional 10-fold. The rate of PNA transfer to solution proceeded at the same rate as transfer to unlabeled vesicles. At low pH, the kinetics of partitioning of the probe could not be accurately determined because of the much lower solubility of the protonated PNA in the aqueous buffer. The results summarized in Table I indicated that the observed first-order process was a rate-limiting dissociation of PNA into buffer, followed by rapid adsorption of the probe into unlabeled acceptor vesicles.

Dependence of PNA Transfer on the Chemical Composition and Physical State of Phospholipid Vesicles. The dependence of the rate of PNA transfer on the physical state and chemical composition of the donor vesicles and independence on those of the acceptor was demonstrated by the data in Table II. At

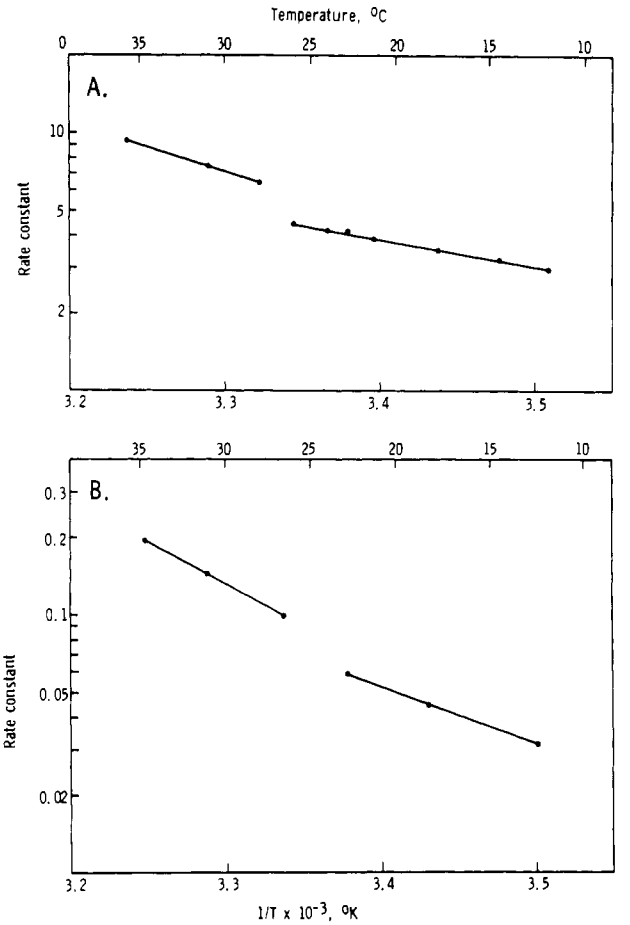

FIGURE 5: Arrhenius plots of PNA transfer between DMPC vesicles. pH 2.8 (A); pH 7.4 (B). The values for the activation energies at pH 7.4 are 9.2 kcal mol^{-1} with DMPC in liquid-crystalline phase and 5.5 kcal mol^{-1} with DMPC in gel phase. The values at pH 2.8 are 13.6 kcal mol^{-1} with DMPC in liquid-crystalline phase and 9.8 kcal mol^{-1} with DMPC in gel phase. All points are the average of five experiments. The stopped-flow instrument and solutions were equilibrated for 30 min at each temperature before equal volumes of donor and acceptor DMPC vesicle concentrations at 0.28 mM were mixed. Donor vesicles contained 2 mol % PNA.

both pH 2.8 and pH 7.4, the transfer rates were characteristic of the donor phospholipid and were the same when either DMPC or DPPC was the acceptor. The rates of transfer from DMPC and DPPC at pH 7.4 were slightly, but reproducibly, different. The transfer of PNA from DPPC at pH 2.8 was more rapid than that from DMPC.

Thermodynamic Parameters of the Activated State. Figure 5 contains Arrhenius plots [ln (rate constant) vs. $1/T$] of the transfer of PNA at both pH 2.8 and pH 7.4. These were reproducibly linear above and below the transition temperature of DMPC, with a discontinuity appearing between 23 and 26 °C. These data, along with kinetic parameters of the activated state calculated by the Eyring formalism (Glasstone et al., 1941), are summarized in Table III. All values were extrapolated to 24 °C, the transition temperature of DMPC. At pH 7.4, activation energies of 9.2 kcal mol^{-1} were obtained when the donor vesicle was in the liquid-crystalline (fluid) state. A value of 5.5 kcal mol^{-1} was determined when the donor was in the gel (solid) state. At pH 7.4, activation energies of 13.6 and 9.8 kcal mol^{-1}, respectively, were calculated for the rate of transfer of PNA above and below the gel → liquid-crystalline transition temperature of DMPC. Duplicate values of the activation energies agreed within 0.3 kcal mol^{-1}, although individual rate constants varied approximately 10–50% between vesicle preparations for transfer of the PNA

Table III: Thermodynamics of the Activated State[a]

	values at pH 7.4	values at pH 2.8	ionization-dependent values
liquid-crystalline phase	$k = 5.4\ s^{-1}$ $E_a = 9.2$ kcal mol^{-1} $\Delta H^{\ddagger} = 8.6$ kcal mol^{-1} $\Delta S^{\ddagger} = -26$ cal deg^{-1} mol^{-1} $\Delta G^{\ddagger} = 16.3$ kcal mol^{-1} (VII) $K^{\ddagger}_{eq} = 8.7 \times 10^{-13}$	$k = 0.08\ s^{-1}$ $E_a = 13.6$ kcal mol^{-1} $\Delta H^{\ddagger} = 13.0$ kcal mol^{-1} $\Delta S^{\ddagger} = -19.5$ cal deg^{-1} mol^{-1} $\Delta G^{\ddagger} = 18.8$ kcal mol^{-1} (I) $K^{\ddagger}_{eq} = 1.3 \times 10^{-14}$	$k(7.4)/k(2.8) = 67.5$ $E_a^{pH} = -4.4$ kcal mol^{-1} $\Delta\Delta H^{\ddagger} = -4.4$ kcal mol^{-1} $\Delta\Delta S^{\ddagger} = -6.5$ cal deg^{-1} mol^{-1} $\Delta\Delta G^{\ddagger} = -2.5$ kcal mol^{-1} $K^{\ddagger}_{eq}(7.4)/K^{\ddagger}_{eq}(2.8) = 67$
gel phase	$k = 4.2\ s^{-1}$ $E_a = 5.5$ kcal mol^{-1} $\Delta H^{\ddagger} = 4.9$ kcal mol^{-1} $\Delta S^{\ddagger} = -39$ cal deg^{-1} mol^{-1} $\Delta G^{\ddagger} = 16.5$ kcal mol^{-1} (VII) $K^{\ddagger}_{eq} = 6.8 \times 10^{-13}$ k(liquid crystalline)/k(gel) = 1.3	$k = 0.062\ s^{-1}$ $E_a = 9.8$ kcal mol^{-1} $\Delta H^{\ddagger} = 9.2$ kcal mol^{-1} $\Delta S^{\ddagger} = -32.8$ cal deg^{-1} mol^{-1} $\Delta G^{\ddagger} = 19.0$ kcal mol^{-1} (I) $K^{\ddagger}_{eq} = 1.0 \times 10^{-14}$ k(liquid crystalline)/k(gel) = 1.3	$k(7.4)/k(2.8) = 67.7$ $E_a^{pH} = -4.3$ kcal mol^{-1} $\Delta\Delta H^{\ddagger} = -4.3$ kcal mol^{-1} $\Delta\Delta S^{\ddagger} = -6.2$ cal deg^{-1} mol^{-1} $\Delta\Delta G^{\ddagger} = -2.5$ kcal mol^{-1} $K^{\ddagger}_{eq}(7.4)/K^{\ddagger}_{eq}(2.8) = 68$
phase-dependent values	$E_a^{T_m} = 3.7$ kcal mol^{-1} $\Delta\Delta H^{\ddagger} = 3.7$ kcal mol^{-1} $\Delta\Delta S^{\ddagger} = -13$ cal deg^{-1} mol^{-1} $\Delta\Delta G^{\ddagger} = -0.2$ kcal mol^{-1} K_{eq}(liquid crystalline)/K_{eq}(gel) = 1.3	$E_a^{T_m} = 3.8$ kcal mol^{-1} $\Delta\Delta H^{\ddagger} = 3.8$ kcal mol^{-1} $\Delta\Delta S^{\ddagger} = -13$ cal deg^{-1} mol^{-1} $\Delta\Delta G^{\ddagger} = -0.2$ kcal mol^{-1} K_{eq}(liquid crystalline)/K_{eq}(gel) = 1.3	

[a] Rate constants were extrapolated to 24 °C, the midpoint of the DMPC transition. Activation energies, E_a, were calculated from the slopes of the Arrhenius plots (Figure 7). Values for $\Delta H^{\ddagger}$, enthalpy of formation of the activated state, were calculated as $\Delta H^{\ddagger} = E_a - RT$. Values for $\Delta S^{\ddagger}$, entropy of formation of the activated state, were calculated from $\Delta S^{\ddagger} = 2.303R \log NhX/(RT)$ where R is the gas constant, T is the temperature in kelvin, k is the reaction rate constant extrapolated to 24 °C, N is Avogadro's number, h is the Planck constant, and X = (rate k)/$e^{-\Delta H^{\ddagger}/RT}$. Values for $\Delta G^{\ddagger\circ}$, the free energy of formation of the activated state, are calculated as $\Delta G^{\ddagger\circ} = \Delta H^{\ddagger} - T\Delta S^{\ddagger}$. Values for $K^{\ddagger}_{eq}$, the equilibrium constant between ground and activated states, are taken from the relationship $K^{\ddagger}_{eq} = -\Delta G^{\ddagger\circ}/(RT)$.

anion and approximately 10% for the transfer of the protonated form of PNA.

Distribution Coefficients of PNA between Vesicles and Buffer. Distribution coefficients of PNA between phospholipid and buffer were determined to compare the free energy changes associated with formation of the kinetic transition state and those associated with aqueous solubilization of PNA. Equilibrium dialysis of [^{3}H]PNA was attempted but was unsuccessful. At acidic pH values, the rate of dialysis from DMPC vesicles was very slow. In addition, the vesicles deteriorated during the several days required for equilibration of the probe. As an alternative experimental method, the distribution coefficients were obtained from changes in the I_E/I_M ratio that resulted from dilution of labeled vesicles into aqueous solutions containing Br^- (Badley, 1976). Bromide ion, 150 mM in the aqueous phase, quenched the fluorescence of aqueous, but not phospholipid bound, fluorophore. From this decrease in the I_E/I_M ratio, the concentration of aqueous PNA was calculated, since the total PNA concentrations were known and the experiment defined the concentration of the probe in the phospholipid matrix. Distribution coefficients and the unitary free energy change associated with solvation of PNA in the bulk phase were calculated from the equations

$$f = X_{aqueous}/X_{membrane} \quad (2)$$

$$\Delta G^{\circ} = -RT \ln f \quad (3)$$

where f is the distribution coefficient, X is the mole fraction of PNA, ΔG° is the free energy change, and R and T have the usual meaning.

Since the mole fraction of PNA in DMPC at any given dilution was obtained by comparison with an initial I_E/I_M ratio before dilution, it was assumed that essentially all of the PNA was membrane bound at the highest concentration. By iterative approximations of the actual amount bound at the highest concentrations, it was shown that this assumption in the least favorable case was valid within approximately 3%. The values calculated from one such set of experiments are listed in Table IV. These data showed that the ΔG° values were considerably lower than the energies required to form the activated state.

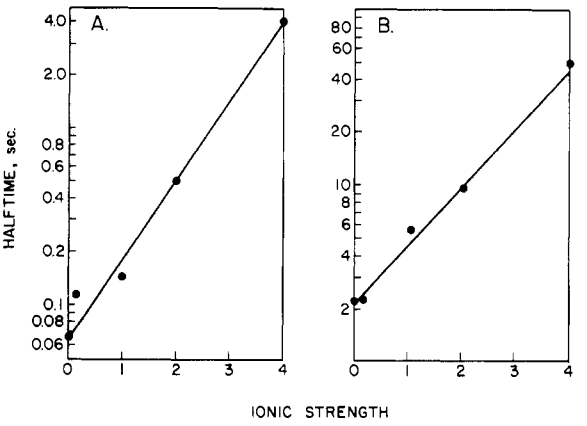

FIGURE 6: Effect of ionic strength on transfer rates. DMPC concentrations were 0.28 mM. Donor vesicles contained 2 mol % PNA. Reactions at pH 9.0 (A) were done at 40 °C; those at pH 2.8 (B) were done at 37 °C.

Decrease in PNA Transfer by High Ionic Strength. High ionic strength decreased the rate of PNA transfer at both high and low pH values (Figure 6). The rate of transfer appeared to be an exponential function of ionic strength at both pH 9.0 and pH 3.0, with a 60-fold and 23-fold decrease, respectively, as the ionic strength was increased to 4 M NaCl. There were no gross differences in vesicle structure, assessed by the increase in light scattering by visual inspection of the different solutions, in agreement with ultracentrifugal experiments (Huang & Charlton, 1971).

The transfer of PNA from donor to acceptor DMPC was very slow when phospholipid multilayers were used. The time-dependent decrease in I_E/I_M was complete after ~50 min (Figure 7). A log plot of the same data was not linear and indicated that the overall transfer was not a first-order process.

Discussion

PNA is a fluorescent fatty acid that, like other excimer-forming compounds, has spectral properties that depend on

Table IV: Determination of PNA Distribution between DMPC and Buffer by Dilution[a]

[DMPC] (M)	$[PNA]_{total}$ (M)	I_E/I_M	X_{memb}	X_{aq}	f	ΔG° (kcal mol^{-1})
			Conditions: 37 °C; pH 9.0			
5.71×10^{-4}	1.14×10^{-5}	0.500	2×10^{-2}		–	–
1.14×10^{-4}	2.29×10^{-6}	0.429	1.72×10^{-2}	5.85×10^{-9}	3.4×10^{-7}	9.17
2.29×10^{-5}	4.57×10^{-7}	0.353	1.41×10^{-2}	2.42×10^{-9}	1.7×10^{-7}	9.60
4.57×10^{-6}	9.14×10^{-8}	0.183	3.66×10^{-3}	1.04×10^{-9}	2.9×10^{-7}	9.27
9.14×10^{-7}	1.83×10^{-8}	0.064	1.27×10^{-3}	3.08×10^{-10}	2.4×10^{-7}	9.39
					average	9.36
			Conditions: 37 °C; pH 2.8			
5.71×10^{-4}	1.14×10^{-5}	0.6996	2×10^{-2}		–	–
1.14×10^{-4}	2.28×10^{-6}	0.644	1.84×10^{-2}	3.24×10^{-9}	1.8×10^{-7}	9.58
2.29×10^{-5}	4.57×10^{-7}	0.608	1.74×10^{-2}	1.08×10^{-9}	6.2×10^{-8}	10.22
4.57×10^{-6}	9.14×10^{-8}	0.527	1.51×10^{-2}	4.06×10^{-10}	2.69×10^{-8}	10.74
9.14×10^{-7}	1.83×10^{-8}	0.368	1.05×10^{-2}	1.56×10^{-10}	1.49×10^{-8}	11.10
					average	10.40
			Conditions: 15 °C; pH 9.0			
5.71×10^{-4}	1.14×10^{-5}	0.333	2×10^{-2}		–	–
1.14×10^{-4}	2.28×10^{-6}	0.304	1.83×10^{-2}	3.67×10^{-9}	2.0×10^{-7}	8.80
2.29×10^{-5}	9.14×10^{-7}	0.266	1.60×10^{-2}	1.65×10^{-9}	1.0×10^{-7}	9.18
4.57×10^{-6}	9.14×10^{-8}	0.152	9.10×10^{-3}	8.98×10^{-10}	9.9×10^{-8}	9.20
9.14×10^{-7}	1.83×10^{-8}	0.080	4.78×10^{-3}	2.51×10^{-10}	5.3×10^{-8}	9.56
					average	9.18
			Conditions: 15 °C; pH 2.8			
5.71×10^{-4}	1.14×10^{-5}	0.304	2×10^{-2}		–	–
1.14×10^{-4}	2.28×10^{-6}	0.295	1.94×10^{-2}	1.216×10^{-9}	5.7×10^{-8}	9.51
2.29×10^{-5}	4.57×10^{-7}	0.291	1.914×10^{-2}	3.52×10^{-10}	1.8×10^{-8}	10.18
4.57×10^{-6}	9.14×10^{-8}	0.282	1.86×10^{-2}	1.19×10^{-10}	6.5×10^{-9}	10.75
9.14×10^{-7}	1.83×10^{-8}	0.229	1.51×10^{-2}	8.13×10^{-11}	5.4×10^{-9}	10.86
					average	10.33

[a] DMPC vesicle solutions with 2 mol % PNA were prepared at 0.57 mM in buffers containing 0.15 M NaBr. After serial fivefold dilutions, ethanol concentrations were adjusted to 2% w/v for all solutions. Spectra were recorded on the SLM photon-counting instrument. Instrument response was fixed for each solution by adjustment of the excitation slit width (range 250–2000 μm). The accumulation times were 1 s/increment at monomer wavelengths and 2 s/increment at excimer wavelengths. Solutions were equilibrated at the desired temperature for 1 h in a separate bath before spectra were recorded and then equilibrated for 10 min within the machine. X_{memb}, mole fraction of PNA in DMPC, was calculated from the relationship $X_{memb} = (I_E/I_M)/(I_E/I_M)_0(2 \times 10^{-2})$. X_{eq}, the mole fraction of PNA in buffer, was calculated from the relationship $X_{aq} = [1 - (I_E/I_M)/(I_E/I_M)_0]([PNA]_{total})(1/55.5)$. It was assumed that partitioning was negligible at the highest vesicle concentration. The distribution coefficient f was calculated as the ratio $f = X_{aq}/X_{memb}$. The unitary free energy of transfer into buffer, ΔG°, was calculated from the relationship $\Delta G^\circ = -RT \ln f$ and is expressed in kcal mol^{-1}. No hydrolysis of DMPC at either pH was noted by thin-layer chromatography.

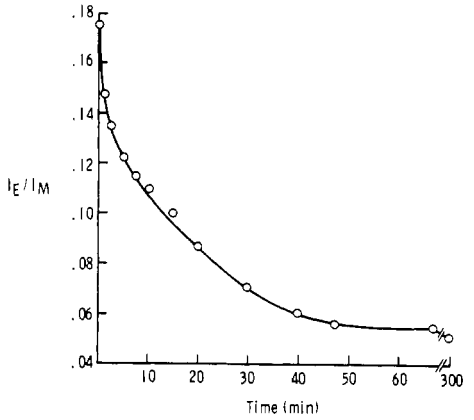

FIGURE 7: PNA transfer between DMPC multilayers. Donor and acceptor multilayers were prepared at 1 mg mL^{-1} DMPC and used at 32.5 °C; pH 7.4, after removal of small amounts of precipitated lipid by centrifugation. Donor multilayers contained 2 mol % PNA.

microscopic concentration and the microviscosity of the environment. At relatively low probe concentrations, the relative excimer fluorescence as expressed by the quantity I_E/I_M decreases with both an increase in the average volume that confines each PNA molecule and an increase in the viscosity of the probe microenvironment. Only volume changes are important in this study. In addition, since only net transfer of the probe is observed, this experimental approach is not complicated by exchange processes.

PNA equilibrates spontaneously with the larger phospholipid volume that becomes available when unlabeled vesicles are introduced in the reaction mixture. The kinetics of transfer are first order under all conditions, as determined from the time-dependent exponential decay of excimer fluorescence. The transfer rates are independent of the chemical composition of the acceptor vesicles. In addition, the kinetic parameters are independent of donor and acceptor vesicle concentration over a 50-fold concentration range. A concentration dependence would be expected if the transfer mechanism involves a transient donor–acceptor "collision complex" (Gurd, 1960), within which subsequent equilibration of fatty acid occurs. The rate-limiting step cannot involve a physical contact by collision or transient fusion of donor and acceptor particles.

A value for the pK_a of PNA in the phospholipid vesicle can be determined from the pH dependence of the rates of transfer. Since the equilibration of the proton between the two forms of membrane-bound fatty acid is much faster than the transfer step (Eigen et al., 1964), the observed rate of total PNA transfer at any pH is the arithmetic sum of the individual first-order transfer rates for the protonated and unprotonated forms at that pH.

The individual rate constants calculated from the half-times of transfer of protonated and ionized PNA at pH 2.8 and 7.4 are 0.17 and 15.9 s^{-1}, respectively. The accuracy of the value determined for the midpoint of a plot of the observed rate, k, vs. pH is limited by the accuracy of the determinations for the transfer rates. These rates are much faster at higher pH and

influenced to a greater extent by the instrumental artifacts associated with fast reactions. The observed transfer rate at higher pH values varied 10–50% with different vesicle preparations. The pH at which transfer of both forms of PNA is equal is pH 5.1, i.e.

$$k_{HA}[HA] = k_{A^-} - [A^-] \quad (4)$$

Since the rate constants k_{HA} and k_{A^-} differ ~100-fold[2] at this pH, the concentration of HA is about 100 times greater than that of A^-. The $pK_{a(memb)}$ of PNA in the surface is 7.1, calculated by the algebraic substitution into the Henderson–Hasselbalch formulation. Suppression of the ionization of probes in membranes and monolayers is well-known (Rigaud et al., 1977; Fernandez & Fromherz, 1977; Fromherz, 1973). A comparison of experimentally determined and theoretically derived half-times is presented in Figure 4. The agreement between these values lends considerable credence to the values given for k_{A^-}, k_{HA}, and $pK_{a(memb)}$. We calculate that less than 1% of PNA transfer at pH 2.8 occurs as the ionized fatty acid and less than 1% of PNA transfer at pH 7.4 occurs as the protonated form.

The linearity and extent of transfer of PNA from single-walled vesicles indicates that flip-flop of the probe is much faster than the rate-limiting step of transfer to the aqueous phase, unless all of the probe in single bilayer vesicles was asymmetrically associated with the exterior leaflet. The method of vesicle preparation makes such an asymmetry improbable. In addition, when unlabeled vesicles were mixed with an aqueous solution of PNA, excimer fluorescence increased within the mixing time of the stopped-flow instrument to a value identical with that obtained when DMPC and PNA were combined before vesicle preparation. Transbilayer flip-flop, therefore, cannot be invoked to explain the nonlinear and greatly reduced rate of transfer observed with multilamellar liposomes. For the transfer of sufficient probe to decrease the I_E/I_M ratio, a large number of consecutive transfers would be required for movement of the probe from the inner to outer layers. Because of the relatively slow desorption of PNA from a phospholipid surface, serial transfer from the individual lamelli to the aqueous interstitial spaces can account for the observed reduction in the transfer rate in multilayer systems, particularly at the lower pH values likely to be present in unbuffered solution between bilayers (Sengupta et al., 1976).

The rate-limiting step could be transfer of PNA from the donor vesicle either to the aqueous phase or through an artificial barrier. These kinetic experiments indicate that transfer through the aqueous phase is the rate-limiting step; however, since the free energy changes associated with formation of the kinetic transition state are greater than those associated with aqueous solubilization (Table IV), there must be a rate-determining energy barrier over which PNA must pass prior to solvation of the bulk aqueous phase. At least two alternatives are possible. The first is that some transient and energetically unfavorable process must occur within the bilayer itself, which is a necessary condition for exit into the aqueous phase. The second is that some property of the bound water structure immediately adjacent to the bilayer surface is the responsible factor. If the first hypothesis were valid, experimental manipulations which have an effect on the solubility of hydrophobic compounds in water should have no major effect on transfer rates, whereas these should have a profound effect upon the transfer rates if solubility of the PNA in the interfacial water is the limiting factor in transfer. The salt effect strongly supports the latter hypothesis.

Another relevant finding is the pronounced effect of high concentrations of NaCl (Figure 7), which decreases the solubility of hydrophobic compounds in water (Long & McDevit, 1952). The markedly slower transfer rates are interpreted to reflect a "salting-out" effect that changes the equilibrium between the phospholipid-bound and activated states. The magnitude of the effect excludes possible rearrangement of the lipid matrix as the rate-limiting step and strongly suggests that entry into the interfacial water is rate determining. In support of this possibility is the observation of Huang & Carlton (1971) that bulk aqueous phase solutes are partially excluded from the interfacial environment of sonicated phospholipid vesicle preparations. The effect of ionic strength suggests that the solvation properties of the interfacially bound water of the donor vesicles may limit the kinetics of transfer of hydrophobic molecules.

To ascertain the possible location of the transition state in this kinetic scheme, we calculated the free energies of the transition state, compared to the ground state in the phospholipid matrix, from kinetic parameters (Table III) for the four experimental conditions involving the two phase states of the phospholipid matrix and the two states of ionization of PNA.

Inspection of the thermodynamic quantities of the activated state reveals that some terms depend upon the ionization state of PNA but not upon lipid phase, i.e., carboxyl group dependent parameters, and vice versa, i.e., hydrocarbon group dependent parameters.

Ionization-Dependent, Phase-Independent Parameters. The differences in activation energies and enthalpies for the formation of the activated state of protonated fatty acid above and below the transition temperature are remarkably similar, −4.4 kcal mol^{-1} for the liquid-crystalline phase and −4.3 kcal mol^{-1} for the gel phase. These energies are interpreted to reflect a difference in the heat of solubilization of the protonated and ionized carboxyl group in the interfacial water. Since very little enthalpy change is associated with the ionization of carboxylic acids in water (Daniels & Alberty, 1975), this excess heat is postulated as a requirement to overcome a phospholipid surface mediated, but lipid phase independent, stabilization of the protonated form, involving the phosphate moiety of the phosphatidylcholine.

The differences in the entropy change needed for formation of the activated state of the protonated and the ionized form of PNA, above and below the lipid transition, are also comparable, −6.5 cal deg^{-1} mol^{-1} for the liquid-crystalline phase and −6.2 cal deg^{-1} mol^{-1} for the gel phase. The interpretation of these entropic values is less certain. No information is available on the role of the carboxyl counterion in the transfer of the ionized form. The contribution of the counterion would likely be a major determinant of the entropy of the activated state.

Because of the similarity of the ionization-dependent, phase-independent values of $\Delta\Delta H^{\ddagger}$ and $\Delta\Delta S^{\ddagger}$, it follows that the corresponding $\Delta\Delta G^{\ddagger}$ values for the protonated and unprotonated transition states are nearly equal. The value is −2.5 kcal mol^{-1} in both phases, from which pK_a of PNA in the phospholipid vesicle is calculated to be 1.8 pH units greater than that of the activated state. Since the $pK_{a(memb)}$ of PNA is about 7.1 by kinetic criteria, the pK_a of the transition-state molecule should be approximately pH 5.3.

Phase-Dependent, Ionization-Independent Kinetic Parameters. There is also an apparent identity in the differences in the kinetic parameters for both ionization states for transfer

[2] These variations in rate constants introduce errors of about 200 cal mol^{-1} in the calculated value of $\Delta G^{\ddagger}$ and 1 cal deg^{-1} mol^{-1} for $\Delta S^{\ddagger}$.

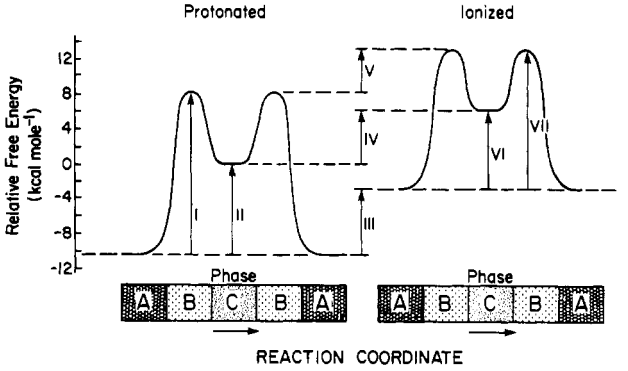

FIGURE 8: Correlation of pH and phase dependence with thermodynamic quantities. Energy level diagrams are discussed in the text for the transfer of PNA between DMPC vesicles in the liquid-crystalline phase at 37 °C and in the gel phase at 15 °C. Phases A, B, and C denote the phospholipid vesicle, the interfacial region, and the aqueous phase, respectively. The experimental values for I, found in Table III, are 18.8 and 19.0 kcal mol^{-1} for the liquid-crystalline and gel phases, respectively. The experimental values for VII, also found in Table III, are 16.3 and 16.5 kcal mol^{-1} for the liquid-crystalline and gel phases, respectively. The values for II, found in Table IV, are 10.4 and 10.3 kcal mol^{-1} for the liquid-crystalline and gel phases, respectively; for VI, the respective values are 9.4 and 9.2 kcal mol^{-1}. Differences in the relative free energies between the protonated and ionized PNA are compared for the phospholipid phase (III), the aqueous phase (IV), and the interfacial phase (V).

from both lipid phases. These differences are 3.8 kcal mol^{-1} at pH 2.8 and 3.7 kcal mol^{-1} at pH 7.4. It appears that the enthalpy originally required to fit the PNA hydrocarbon group into the gel-phase crystalline lattice of DMPC as an impurity is available to the system as PNA leaves the membrane system to the interfacial aqueous phase. Supporting this postulate is the experimental observation that the molar enthalpy of crystallization in DMPC is approximately 5.4 kcal mol^{-1} (Mabrey & Sturtevant, 1976). Any crystallization process at the melting point of the system is accompanied by a corresponding decrease in entropy:

$$\Delta G^\circ = \Delta H - T\Delta S = 0 \quad (5)$$

$$\Delta H = T\Delta S \quad (6)$$

The molar entropy of crystallization in DMPC is 18.2 cal deg^{-1} mol^{-1}. When the temperature is that of the transition temperature, the entropy of activation would be 13 cal deg^{-1} mol^{-1} less at both pH 7.4 and pH 2.8 for transfer from the gel phase, compared to the liquid-crystalline phase. This result gives an overall difference in $\Delta G^\ddagger$ of only around −0.2 kcal mol^{-1} for transfer of either form of probe at the transition temperature from the gel phase, compared to the liquid-crystalline phase. These findings raise an interesting possibility that crystallization of the lipid matrix and entry of hydrophobic compounds into the interfacial aqueous phase are concerted and complementary processes.

Construction of Energy Level Diagrams. If a pK_a of 5.0 for PNA is assumed as reference for a monomer species in the bulk aqueous phase, energy level diagrams for the reaction can be constructed to relate directly the free energy of both ionization forms of PNA when the fatty acid is in the phospholipid phase, in the rate-determining interfacial aqueous phase, and in the bulk aqueous phase along arbitrary reaction coordinates. Figure 8 is a diagram for the cases of PNA transfer from DMPC in the gel phase at 15 °C and in the liquid-crystalline phase at 37 °C. The differences in the free energies for the two ionization states of interfacial and membrane-bound PNA allow the independent calculation of pK_a values of 3.7 (interfacial) and 5.7 (membrane bound) at 37 °C and 4.0 (interfacial) and 5.9 (membrane bound) at 15 °C. Although the membrane-bound pK_a values do not agree exactly with the value calculated for 24 °C from kinetic parameters only, the aqueous character of the transition-state pK_a and the elevated pK_a of the membrane-bound form are still apparent. Inaccuracies in the determination of the four phospholipid–buffer distribution coefficients almost certainly contribute to these minor discrepancies.

Summary and Conclusions

The exchange of PNA between DMPC bilayer vesicles is a first-order process in which the rate-limiting step is dissociation from the donor vesicle into the aqueous phase, followed by a much faster diffusion to and uptake by a neighboring acceptor vesicle. Analysis of the thermodynamics of the activated state and of partitioning indicates that formation of an aqueous intermediate in the interfacial region is the rate-limiting step. Crystallization forces in the artificial membrane appear to contribute energy to the formation of this activated state. The most significant and interesting aspect of this work is the finding that the kinetics of exchange of hydrophobic compounds between lipid structural entities is a process which is not rigidly dictated by partition equilibrium and may be amenable to catalysis by changes in the solvation properties of interfacial water.

Acknowledgments

We thank Phyllis Gutierrez and Sharon Bonnot for preparation of the manuscript. We are indebted to Dr. L. A. Sklar for the gift of *β-all-trans*-parinaric acid. We are also most grateful to Dr. S. C. Charlton for many helpful discussions and Dr. Dominic Desiderio for performing the mass spectroscopy.

References

Almgren, M., Grieser, F., & Thomas, J. K. (1979) *J. Am. Chem. Soc. 101*, 279–291.

Badley, R. A. (1976) in *Modern Fluorescence Spectroscopy* (Wehry, E. L., Ed.) Vol. 2, pp 91–168, Plenum Press, New York.

Bangham, A. D., Standish, M. M., & Watkins, J. C. (1965) *J. Mol. Biol. 13*, 238–252.

Batzri, S., & Korn, E. D. (1973) *Biochim. Biophys. Acta 198*, 1015–1019.

Birks, J. B. (1970) *Photophysics of Aromatic Molecules*, pp 301–371, Wiley-Interscience, New York.

Charlton, S. C., Olson, J. S., Hong, K.-Y., Pownall, H. J., Louie, D. D., & Smith, L. C. (1976) *J. Biol. Chem. 251*, 7952–7955.

Charlton, S. C., Hong, K.-Y., & Smith, L. C. (1978) *Biochemistry 17*, 3304–3309.

Daniels, F., & Alberty, R. A. (1975) *Physical Chemistry*, 4th ed., p 228, Wiley, New York.

Doody, M. C., Pownall, H. J., & Smith, L. C. (1978) *Fed. Proc., Fed. Am. Soc. Exp. Biol. 37*, 1832.

Eigen, M., Kruse, W., Mass, G., & DeMaeyer, L. (1964) *Prog. React. Kinet. 2*, 285.

Fernandez, M., & Fromherz, P. (1977) *J. Phys. Chem. 81*, 1755–1761.

Fromherz, P. (1973) *Biochim. Biophys. Acta 323*, 326–334.

Galla, H.-J., & Sackman, E. (1974) *Biochim. Biophys. Acta 339*, 103–115.

Glasstone, S., Laidler, K., & Eyring, E. (1941) *The Theory of Rate Processes*, p 100, McGraw-Hill, New York.

Gurd, F. (1960) in *Lipide Chemistry* (Hanahan, D., Ed.) p 283, Wiley, New York.

Huang, C., & Carlton, J. (1971) *J. Biol. Chem. 246*, 2555–2560.
Kao, Y. J., Charlton, S. C., & Smith, L. C. (1977) *Fed. Proc., Fed. Am. Soc. Exp. Biol. 56*, 936.
Long, F. A., & McDevit, W. R. (1952) *Chem. Rev. 51*, 119–169.
Mabrey, S., & Sturtevant, J. M. (1976) *Proc. Natl. Acad. Sci. U.S.A. 73*, 3863–3866.
Patel, K. M., & Sparrow, J. T. (1978) *J. Chromatogr. 150*, 542–547.
Patel, K. M., Pownall, H. J., Morrisett, J. D., & Sparrow, J. T. (1976) *Tetrahedron Lett. 45*, 4015–4018.
Pownall, H. J., & Smith, L. C. (1974) *Biochemistry 13*, 2594–2597.
Rigaud, J., Cary-Bobo, C., Sanson, A., & Ptak, M. (1977) *Chem. Phys. Lipids 18*, 23–38.
Robinson, D. S. (1970) *Compr. Biochem. 18*, 51–116.
Scow, R. O., Hamosh, M., Blanchette-Mackie, E. J., & Evans, A. J. (1972) *Lipids 7*, 497–505.
Sengupta, P., Sackmann, E., Juhnle, W., & Scholz, J. P. (1976) *Biochim. Biophys. Acta 436*, 869–878.
Sklar, L., Hudson, B. S., & Simoni, R. (1977) *Biochemistry 16*, 819–825.
Smith, L. C., & Scow, R. D. (1979) *Prog. Biochem. Pharmacol. 15*, 65–91.
Soutar, A. K., Pownall, H. J., Hu, A., & Smith, L. C. (1974) *Biochemistry 13*, 2828–2836.
Vanderkooi, J., & Callis, J. (1974) *Biochemistry 13*, 4000–4006.
Van Dijck, P., De Kruijff, B., Aarts, P., Verkleij, A., & De Gier, J. (1978) *Biochim. Biophys. Acta 506*, 183–191.

Fluorine-19 Nuclear Magnetic Resonance Investigation of the Noncovalent and Covalent Binary Complexes of 5-Fluorodeoxyuridylate and *Lactobacillus casei* Thymidylate Synthetase†

Charles A. Lewis, Jr.,‡ Paul D. Ellis,§ and R. Bruce Dunlap*

ABSTRACT: Formation of the 5-fluorodeoxyuridylate–thymidylate synthetase binary complex produced ^{19}F NMR resonances 1.4 and 34.5 ppm to higher shielding of free nucleotide. Denaturation demonstrated that the greatly shifted resonance represented nucleotide covalently attached to the enzyme and afforded narrowing of the resonance so that it could be resolved into a doublet and a singlet. Comparison with ^{19}F NMR spectra of bisulfite adducts of 5-fluorodeoxyuridine and 5-fluorodeoxyuridylate permitted identification of the covalent species as the 5,6-dihydro derivative of 5-fluorodeoxyuridylate which is linked to the catalytic cysteine in the active site of the enzyme. The doublet and singlet resonances of the dihydro species result from the H_2O/D_2O content of the buffer which produced an isotope-shifted ^{19}F resonance for the deuterated species. The enzyme appears to stereoselectively produce a single isomer of the covalent binary complex. The extent of complex formation was observed to be dependent upon the concentration of phosphate present in solution, with high concentrations disfavoring complex formation. The greatest extent of binary complex formation was found in Tris-HCl buffer. In piperazine-*N*,*N*′-bis(2-ethanesulfonic acid) (Pipes) buffer, significantly increased resolution of the resonance for the covalent species was obtained upon addition of less than an equivalent amount of phosphate to the binary complex. This permitted direct observation of the 5,6-dihydro species resonance in the native binary complex. Binding of 5-fluorodeoxyuridylate to thymidylate synthetase occurs as an equilibrium mixture of two bound forms, a noncovalent Michaelis complex of the inhibitor with the enzyme and a covalent 5-fluoro-5,6-dihydrodeoxyuridylate–6-enzyme complex.

Studies by numerous investigators permit us to write a moderately detailed chemical mechanism for the reductive methylation of dUMP[1] catalyzed by thymidylate synthetase (EC 2.1.1.45) to form dTMP utilizing CH_2H_4folate as the source of the methyl group (Scheme I) (Friedkin, 1973; Danenberg, 1977; Pogolotti & Santi, 1977). The central feature of this mechanism is the formation and breakdown of a 5,6-dihydro derivative of dUMP which is covalently bound to both the enzyme and CH_2H_4folate [(C) of Scheme I]. The catalytic ternary complex results from attack of the active-site cysteine on carbon 6 of dUMP, followed by electrophilic addition at carbon 5 by the methylene group of CH_2H_4folate. Decomposition of this complex is initiated by abstraction of the proton on carbon 5, followed by either a concerted breaking of the remaining bond to the folate with internal hydride transfer (Friedkin, 1959) or formation of an exocyclic methylene group on carbon 5, which then undergoes reduction (Santi et al., 1974).

† From the Department of Chemistry, University of South Carolina, Columbia, South Carolina 29208. *Received May 29, 1979.* This work was supported in part by the National Institutes of Health through Grants CA 12842 and CA 15645 from the National Cancer Institute.

* Correspondence should be addressed to this author. He is the recipient of a Faculty Research Award (FRA-144) from the American Cancer Society.

‡ Recipient of a National Research Service award (CA 06097) from the National Cancer Institute of the National Institutes of Health.

§ A fellow of the A. P. Sloan Foundation.

[1] Abbreviations used: dUMP, deoxyuridylate; dTMP, deoxythymidylate; CH_2H_4folate, (±)-5,10-methylene-5,6,7,8-tetrahydrofolate; FdUMP, 5-fluorodeoxyuridylate; FdU, 5-fluorodeoxyuridine; MMTS, methyl methanethiolsulfonate; Pipes, piperazine-*N*,*N*′-bis(2-ethanesulfonic acid); 5-NO_2dUMP, 5-nitrodeoxyuridylate.

0006-2960/80/0419-0116$01.00/0